Barrier Height, Interface Charge & Tunneling Effective Mass in ALD Al_2O_3/AlN/GaN HEMTs

Satyaki Ganguly, Jai Verma, Guowang Li, Tom Zimmermann, Huili Xing, Debdeep Jena[*]
University of Notre Dame, Department of Electrical Engineering
275 Fitzpatrick, Notre Dame, IN 46556, [*]Email: djena@nd.edu, [*]Phone: 574-631-8835

Atomic layer deposited (ALD) high band gap (~6.5eV) [1], high k (~9.1) Al_2O_3 has emerged as an attractive candidate to support vertical scaling of AlN/GaN HEMTs [2] and its variants owing to its outstanding dielectric, thermal, and chemical properties. Integration of ALD oxides with GaN will enable lower gate leakage currents, high breakdown voltages, and surface passivation. In this work we present a comprehensive characterization of AlN/GaN MOS-HEMT gate stacks with ALD Al_2O_3 of various thicknesses. Through capacitance-voltage and Hall-effect measurements, we find the presence and propose an origin of benign donor-type interface charge (Q_{int}) at the AlN/Al_2O_3 junction, and relate its presence to the polarization charges in AlN. By studying tunneling transport in corresponding (Ni/Al_2O_3/Ni) M-I-M diodes, we extract the Ni/Al_2O_3 surface barrier height (Φ_B), the electron tunneling effective mass in Al_2O_3, and discuss the resulting HEMTs.

ALD/AlN Interface: AlN/GaN HEMT structures with ~4nm barrier were grown by MBE on semi insulating 0001 GaN templates (2μm) on sapphire. Mesa isolation was followed by Ti/Al/Ni/Au stack source/drain alloyed ohmic metallization. The same sample was then cleaved into four parts, and four different Al_2O_3 thicknesses (t_{ox}=2nm, 4nm, 6nm, 8nm) were deposited on the AlN surface by ALD with TMA and H_2O as the precursors. Finally, Ni/Au (50/150 nm) gate metal stacks were deposited simultaneously. The layer structure of the sample is shown in Fig. 1(a). Figure 1(b) & (c) shows the cross-section TEM image of gate stack of the (t_{ox}=4nm) sample, confirming the thicknesses, and shows thickness variations within an acceptable window. Fig. 2(a) shows the capacitance-voltage (C-V) measurement (@1MHz) data for the four samples (they show negligible hysteresis). The pinch-off voltage V_p increases with t_{ox} from -3.5 V for t_{ox}=2nm to -8.8V for t_{ox}=8nm. The carrier profile extracted [3] from the C-V measurement is shown in Fig. 2(b), indicating the varying depth of the 2DEG channel from the gate metal. Fig. 2(c) shows the decreasing gate leakage current with increasing t_{ox}, the property that will enable high breakdown voltages in AlN/GaN HEMTs. The increase in V_p with t_{ox} over the 4 samples can be *quantitatively* explained by the existence of a fixed *positive* sheet charge Q_{int}~6×10^{13} cm^{-2} at the (Al_2O_3/AlN) interface as shown in Fig. 3(a). Self-consistent 1-D Poisson-Schrödinger simulation [4] for Q_{int}=0 cannot explain the experimental data as shown in Fig. 3(a). The Ni/Al_2O_3 surface barrier height used is the measured (see later) value Φ_B=2.9eV. The interface density Q_{int}~6×10^{13} cm^{-2} is remarkably close to the surface polarization charge of a strained AlN layer. We argue that since the AlN surface is metal (Al)-face, in ALD oxygen atoms attach to Al and can be viewed as substituting the nitrogen site [5], thus acting as donor dopants by electron counting rules. The picture is essentially identical to modulation doping: the positive sheet charge at the Al_2O_3/AlN interface [inset, Fig. 3(a)], neutralizes negative polarization charges of the AlN surface, increasing the 2DEG density at the AlN/GaN heterojunction. Fig. 3(b) shows that the increase in the experimental 2DEG density n_s (from C-V) with t_{ox} can be explained if $Q_{int} = 6\times10^{13}$ cm^{-2} is assumed. This finding is verified with another AlN/GaN structure with a thinner AlN barrier. Fig. 3(c) shows the Hall-effect measured charge before and after ALD deposition (t_{ox}=5nm). Charge density loci predicted by Poisson-Schrödinger simulations for various Q_{int} (after ALD) and Φ_B are shown in Fig. 3(c), confirming that $Q_{int} = 6\times10^{13}$ cm^{-2} and Φ_B =2.9eV match the experimental data.

Ni/ALD Interface: Four M-I-M (Ni/ALD Al_2O_3/Ni) diode structures were fabricated with t_{ox}=8, 9, 10, 12nm for Fowler-Nordheim (FN) type tunneling studies. Fig. 4(a) shows the measured tunneling current density (J) vs. the oxide electric field (E_{ox}) for the four samples, and Fig. 4(b) shows the FN plots for the t_{ox}=10 and 12nm samples. From the slope of these plots Φ_B = 2.9eV and an electron tunneling effective mass of $m_T^* \sim 0.16 m_0$ are extracted. This tunneling effective mass is similar to an earlier report [6].

The dc I-V characteristics of the depletion mode HEMT (t_{ox}=6nm) is shown in Fig. 4(c), and Fig. 4(d) shows the transfer characteristics with the gate capacitance. The subthreshold slope SS and V_p extracted from the transport measurement (transfer characteristics) is SS~285mV/decade and V_p=-7.6V are in close agreement with those extracted from the static (no transport) C-V plot (SS~320 mV/decade and V_p=-7.7V). This indicates that the SS is not a transport/short channel effect, but related to the gate stack itself.

The extraction of the polarization-related ALD/AlN interface charge, the Ni/ALD barrier height, and the tunneling effective mass of electrons through ALD Al_2O_3 into AlN/GaN heterojunctions reported here is expected to accelerate the choice of optimal gate stacks for nitride HEMTs. In addition, the role of ALD oxygen layers as possible modulation dopants can be cleverly exploited for novel purposes in nitride electronic devices.

[1]   N. V. Nguyen *et al*, *Appl. Phys. Lett.*, 93, 082105, (2008).
[2]   H. Xing *et al*, *ECS transactions, Vol.*11, (2007).
[3]   N. Onojima *et al*, *J. Appl. Phys.*, 101, 043703, (2007).
[4]   I. H. Tan *et al*, *J. Appl. Phys.*, 68, 4071, (1990).
[5]   T. Mattila *et al*, *Phys. Rev B*, 54, 23, (1996).
[6]   M. D. Groner *et al*, *Thin Solid Films*, 413, (2002).
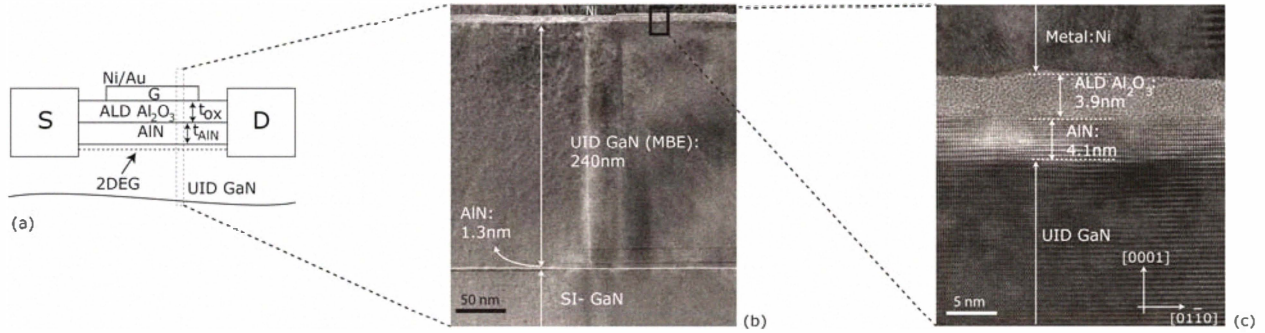
Fig.1 (a) Schematic layer structure of the sample; (b) High Resolution Transmission Electron Microscope image along zone axis [100] showing the layer structure of the sample; (c) High-resolution lattice image of the gate stack showing the crystalline AlN barrier layer, the amorphous ALD Al_2O_3 and Ni as gate metal.
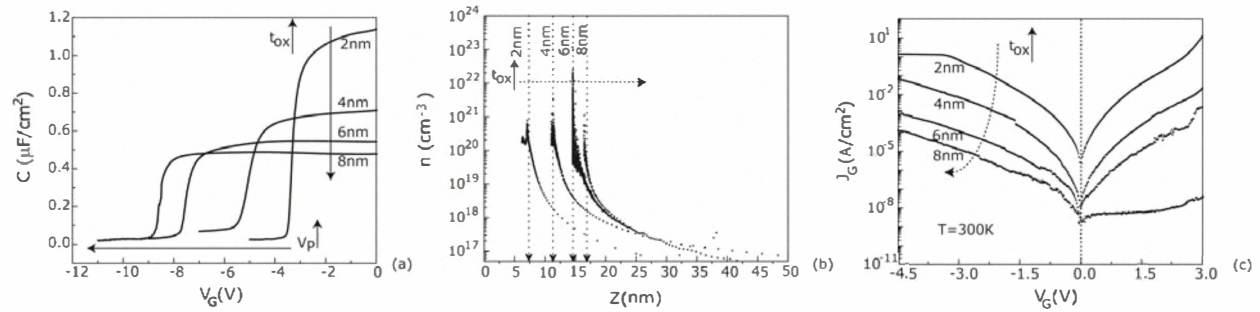
Fig. 2 (a) C-V plots (@1MHz) of the four samples with different t_{ox}, showing V_p increases with increasing t_{ox}; (b) Plots showing the charge profile and varying depth of 2DEG channel from the gate metal for samples with different t_{ox}; (c) Gate leakage current density vs. gate voltage plots indicating the reduction of J_G with increasing t_{ox}.
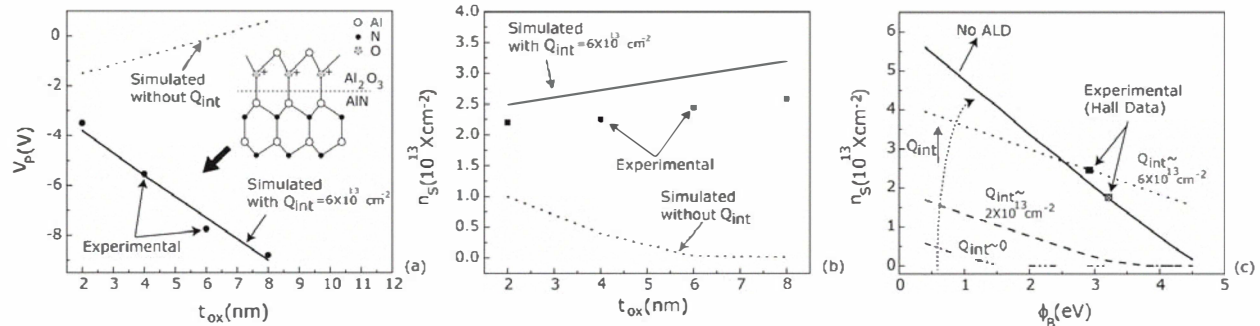
Fig. 3 (a)-(b) Experimental and simulated (w and w/o Q_{int}) V_p and n_s for different t_{ox}. The atomic arrangement at the Al_2O_3/AlN interface and the positive donor dopants giving rise to Q_{int}, are shown in the inset(a); (c) Simulation data plot showing the variation of n_s with Φ_B before and after 5nm ALD (for various Q_{int}). The Hall measured n_s before and after ALD (t_{ox}=5nm) are compared with the simulation result.
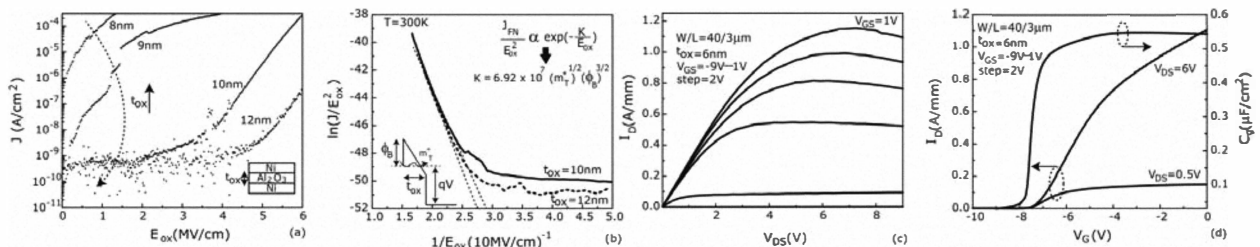
Fig. 4 (a) J versus E_{ox} for the M-I-M structures with different t_{ox}. Inset: Schematic layer structure of the M-I-M diode; (b) FN plots for the samples with t_{ox}=10nm, 12nm. The expression in the inset is used to extract Φ_B & m_T^* from the slope. Schematic band diagram for FN tunneling (@ $qV > \Phi_B$) is shown in the inset; (c) dc I-V characteristics of Al_2O_3/AlN/GaN (6/4/235nm) depletion mode HEMT; (d) Transfer characteristics (for V_{DS}=0.5, 6) and gate capacitance (vs V_G) plot for the Al_2O_3/AlN/GaN (6/4/235nm) HEMT structure.